Journal of Applied Polymer Science

Effect of Noncovalent Chemical Modification on the Electrical Conductivity and Tensile Properties of Poly(methyl methacrylate)/ Carbon Nanotube Composites

Ozcan Koysuren, Mustafa Karaman, Demet Ozyurt
Department of Chemical Engineering, Selcuk University, Konya 42031, Turkey
Correspondence to: M. Karaman (E-mail: karamanm@selcuk.edu.tr) or O. Koysuren (E-mail: koysuren@selcuk.edu.tr)

ABSTRACT: Noncovalent chemical modification by initiated chemical vapor deposition technique is applied to carbon nanotubes (CNTs) to reduce average agglomerate size of the nanoparticles in the polymer matrix and to improve surface interaction between the composite constituents. CNT surfaces are coated conformally with thin poly(glycidyl methacrylate) (PGMA) polymer film and coated nanoparticles are incorporated in poly(methyl methacrylate) (PMMA) polymer matrix using solvent casting technique. Conformal PGMA coatings around individual nanotubes were identified by scanning electron microscopy analysis. Transmission electron microscopy and optical microscopy analyses show homogeneous composite morphology for composites prepared by using PGMA coated nanotubes. Fourier Transform Infrared and X-ray photoelectron spectroscopy analyses show the successful deposition of polymer with high retention of epoxide functionality. PGMA coating of CNTs exhibits improvement in electrical conductivity and tensile properties of PGMA-CNT/PMMA systems when compared with uncoated nanoparticles. © 2012 Wiley Periodicals, Inc. J. Appl. Polym. Sci. 000: 000–000, 2012

KEYWORDS: nanotubes; nanocomposites; mechanical properties; surface modification

Received 23 November 2011; accepted 16 May 2012; published online 00 Month 2012
DOI: 10.1002/app.38062

INTRODUCTION

Carbon nanotubes (CNTs) have been considered as ideal additives for high technology nanocomposite materials due to their extraordinary thermal, electrical, and mechanical properties.[1–4] When CNTs are incorporated to a polymer matrix, electrical, mechanical, and other properties of the composite material may change depending on the properties of individual components, the shape, size and amount of the filler, the morphology of the system, and the interface between the components.[5,6] The major problem in composite preparation is the difficulty of obtaining homogeneous nanotube network throughout the polymer matrix due to agglomeration tendency and hydrophobic surface properties of CNTs. Small agglomerate size and homogeneous distribution of nanoparticles in polymer matrix are crucial to combine the attractive features of CNTs and the polymer matrix. In addition, enhanced surface interaction between the composite constituents is important in terms of the final properties of composites.[7,8]

Several techniques have been applied to enhance the interfacial interaction between composite constituents by decreasing average agglomerate size of the conductive filler. Addition of some surfactants and compatibilizers into CNT/polymer solution during the composite preparation improves the dispersion of nanotubes in the polymer matrix; however the presence of such impurities usually results in decreased mechanical properties.[9] Chemical functionalization of nanotube surfaces before composite preparation emerged to be an efficient method for dispersion and alignment improvement. Nanotubes that are surface-functionalized by matrix polymer were found to be highly soluble in the same matrix and solubility depends on the functional group attached to the grafted polymer.[10–13,14] Atom transfer radical polymerization (ATRP) was used successfully to develop many polymer thin films on nanotube surfaces, and the resulting nanohybrid structures were used for many composite systems.[15] ATRP is a wet process to synthesize acrylic or methacrylic polymers with highly controllable chemistries, however, long production times and impurities caused by solvents and catalysts are the major drawbacks of that process. Chemical vapor deposition (CVD) is a dry alternative to produce polymer thin films with well-controlled chemistry and morphology. The substrates with complex geometries can be coated with high uniformity, without solvent related damages, which are observed in conventional wet processes.[16,17]

In this study, it was aimed to enhance the dispersion of CNTs in poly(methyl methacrylate) (PMMA)/acetone solution

through functionalization of nanotube surfaces by initiated CVD (iCVD) method. Compared with other CNT surface treatment methods, iCVD has many advantages. As depositions are carried out under clean vacuum conditions, iCVD produces clean polymers around nanotubes with stoichiometric compositions. Besides, solvent-related damages on nanotube surfaces can be avoided using all-dry iCVD method, hence sp^2-hybridized sidewalls of nanotubes can be well preserved, which essentially improves the electrical and tensile properties of final composites. Poly(glycidyl methacrylate) (PGMA) was deposited conformally on individual nanotubes by using tertiary butyl peroxide as an initiator. Different from ordinary CVD methods, energy required to start chemical reactions is supplied through resistively heated filaments. Tensile and electrical properties of the nanocomposite thin films prepared from PGMA-functionalized CNTs were observed to be highly improved.

EXPERIMENTAL

CNTs were synthesized by chemical vapor deposition technique in a horizontal quartz tube in a tube furnace (Protherm 12/38/250) from hydrogen and ethylene gases over Fe/Al_2O_3 (Fe/Al = 1 : 1) catalyst at 650°C. Fe/Al_2O_3 catalyst powders were placed in a ceramic boat that was packed into the furnace subsequently. Hydrogen was introduced into the furnace before heating to clean up the system. Then the furnace was heated up to 650°C. When the furnace temperature became stable at 650°C, a mixture of hydrogen and ethylene (1 : 2 volume ratio of hydrogen to ethylene) was fed into the furnace for 30 min. Operating gas flow rate of ethylene was 200 mL/min and its flow was stopped when the system started to cool. However, hydrogen flow was continued until the furnace was cooled to the room temperature.[18] During the deposition, 0.1 g of catalyst powders were used and the total yield was about 0.5 g, including CNTs, amorphous carbon, and catalyst impurities.

To remove the catalyst impurities, as-prepared nanotubes were treated with dilute hydrofluoric acid and hydrochloric acid solutions separately. First, CNTs were treated with 7 M hydrofluoric acid solution for 1 day to remove Al_2O_3 from CNTs. After, they were filtered under vacuum and rinsed with distilled water several times. Afterward, they were treated with 3 M hydrochloric acid solution for 3 h to remove Fe catalyst from CNTs. CNT particles were collected again with filtration under vacuum and rinsed with distilled water until the particles were neutralized. After washing with water, nanotube particles were rinsed with ethanol to extract water. Finally, the resultant nanotube particles, separated from catalyst particles, were dried at 60°C overnight.[18]

CNTs were surface functionalized in a custom-built CVD reactor. Reactor contains 12 parallel tungsten filaments Alfa Aesar (Ward Hill, Massachusetts) that are placed 3 cm above the substrate surface (Figure 1). Temperature of the filaments was kept constant at 250°C, which was measured by directly attaching a K-type thermocouple (Omega, Stamford, Connecticut) to one of the filaments. GMA (Sigma Aldrich, St. Louis, Missouri) was used as received without further purification and fed to the reactor as a vapor, after being vaporized at 65°C in a stainless steel jar. Tert-butyl peroxide (Sigma Aldrich) was vaporized at

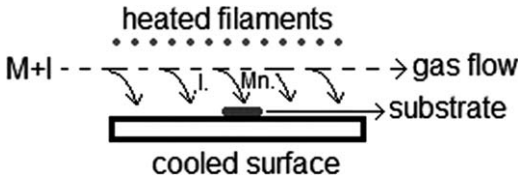

Figure 1. Schematic representation of iCVD process (M: monomer, I: initiator).

room temperature in a glass jar. Monomer and initiator vapors were mixed in a heated pipeline and fed to the reactor through a side port. Flow rates of monomer and initiator were adjusted by needle valves and kept constant at 0.6 and 0.4 sccm, respectively. Vacuum was created by a rotary pump (Edwards, West Sussex, UK). Reactor pressure was measured by a capacitance manometer (MKS, Andover, Massachusetts) and controlled by using a downstream pressure controller (MKS). Nanotubes were agitated during the depositions by placing a magnetic stirrer under the reactor. The temperature of the substrates was kept constant at 25°C by using a water-circulated cooling plate below the substrates. After the coating process, the coated nanotubes (PGMA-CNT) were heat treated in a vacuum oven at 250°C overnight.

PMMA-CNT nanocomposite specimens were prepared by solvent casting method. PMMA (Alfa Aesar) was dissolved in pure acetone to give a 7 % (by weight) solution. In a separate beaker, 50 mg of heat-treated PGMA-CNTs was suspended in 5 mL acetone and resulting solution was ultrasonicated for 6 h. PGMA-CNT/acetone dispersion then was added slowly to the PMMA/acetone solution with continuous mixing by using a magnetic stirrer at 1000 rpm. For comparison purpose, pristine CNT/acetone suspension were prepared and mixed with PMMA/acetone solution. The resulting nanocomposite solutions (PGMA-CNT/PMMA/acetone and CNT/PMMA/acetone) were poured into rectangular aluminum molds and allowed to solidify at room temperature after evaporation of the solvent. Samples with different weight fractions of nanotubes (2, 5, 8 wt %) in PMMA matrices were prepared using exactly the same procedure.

Fourier Transform Infrared (FTIR) spectrophotometer (Model: Perkin Elmer Spectrum 100, Waltham, Massachusetts) was used for chemical characterization of polymer coatings around CNTs. FTIR spectra were recorded between 750 and 4000 cm^{-1} using ATR accessory. Surface chemical compositions of the untreated and coated nanotubes were analyzed by X-ray photoelectron spectroscopy (XPS) (Model: Specs, Berlin, Germany) using a monochromatized Al source. The surface morphology of nanotubes was examined using a scanning electron microscope (SEM) (Model: EVO LS10 Zeiss, Oberkochen, Germany), a transmission electron microscopy (TEM) (Model: Tecnai G2 F30, Hillsboro, Oregon), and an optical microscope (Model: James Swift, Hicksville, New York). The average diameter of CNT fibers was analyzed from the SEM image of untreated CNTs using the National Institutes of Health ImageJ software. High-resolution (1024 × 768 pixels) tif image was used for image analysis. At least 30 different fibers were analyzed and their results were reported as mean ± standard deviation. The

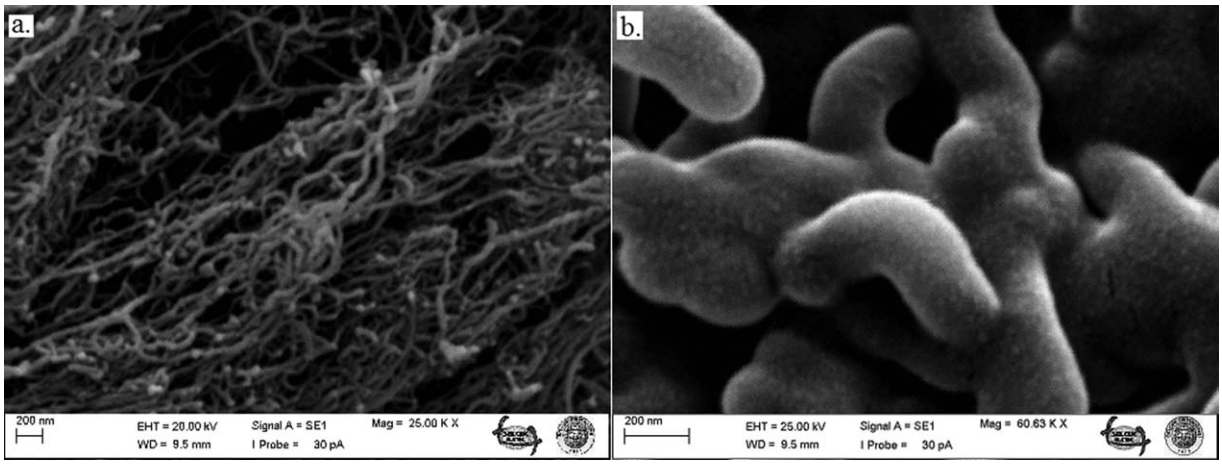

Figure 2. SEM images of (a) pristine CNT and (b) PGMA-coated CNT.

electrical resistivity of CNT/PMMA composites was measured by two-point probe method using a source meter. For a good electrical contact in two-point probe method, copper wires were placed into the solvent-casted composites during sample preparation. Conductivity measurement was performed by contacting probes with these copper wires. The tensile properties of solvent-casted composites were measured using a tensile-testing instrument (Instron 4204 Universal Testing System, Shakopee, Minnesota). Five specimens of each composition were tested and average of these five test results was illustrated with their standard deviations. Solvent-casted specimen had a thickness of 2 mm with a gauge length of 20 mm. According to the gauge length and a strain rate of 0.1 min^{-1}, the crosshead speed of testing instrument was set at 2 mm/min.

RESULTS AND DISCUSSION

Figure 2 shows SEM images of untreated and iCVD-coated CNTs. Pristine nanotubes have average fiber diameter of 28.2 ± 6.8 nm [Figure 2(a)]. After iCVD coating of nanotube surfaces at 450 mTorr reactor pressure and 25°C substrate temperature for 2 h, thick polymer coatings around individual nanotubes can be clearly resolved [Figure 2(b)]. Initiated chemical vapor deposition process follows the guidelines of free radical reaction mechanism; for which, monomer adsorbed physically on the cooled substrate surface polymerize in the presence of free radical initiators. As the attachment of growing polymer chains to the substrate surface occurs at low temperature through physical adsorption mechanism, the interaction between the film and the substrate surface is expected to be noncovalent. Agitation of the nanotube bed during the deposition is believed to increase the film homogeneity and conformability.

Figure 3 shows the FTIR spectra of pristine and PGMA-coated CNTs. The spectrum of pristine nanotubes does not contain significant absorbance peaks compared with the spectrum of PGMA-coated nanotubes, which is expected because CNTs do not absorb much in the infrared region.[19] The weak absorption peaks between 2924 and 2845cm^{-1} can be attributed to —CH stretching, while the peak at 1380 cm^{-1} is due to —CH bending.[20] Relatively stronger peaks at 1720 and 1580 cm^{-1} can be assigned to C=O and C=C bonds.[21] The spectrum of the PGMA-coated nanotubes is totally different than the spectrum of pristine nanotubes. In this spectrum, all characteristic peaks belonging to methacrylate polymers can be clearly resolved: C—H stretching between 3100 and 2800 cm^{-1}, very sharp C=O bond at 1730 cm^{-1}, C—H bending between 1500 and 1350 cm^{-1}, and C—O stretching between 1240 and 1275 cm^{-1}.[19,22,23] Besides, the absence of absorption bands around 1560 cm^{-1} proves that the polymerization proceeded through unsaturated vinyl bonds. The strong absorption peaks at 906, 847, and 759 cm^{-1} are assigned to the epoxide group,[19,22] which proves that iCVD method is capable of producing thin PGMA films around nanotubes without loss of epoxide functionality.

The surface chemical compositions of the pristine and coated CNTs were analyzed by XPS. Survey scan of the pristine CNTs indicated a carbon atomic percentage of 99, together with 1% oxygen. The deconvolution of high-resolution C1s spectrum gives four different carbon sates [Figure 4(a)]. The high-

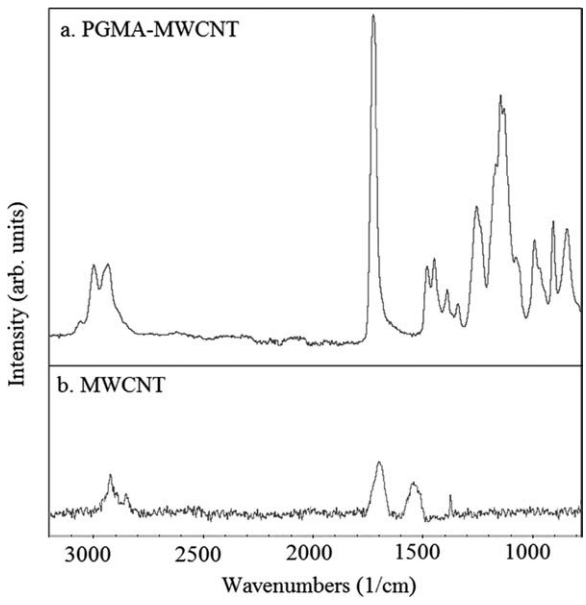

Figure 3. FTIR spectra of (a) PGMA-CNT and (b) pristine CNT.

Applied Polymer SCIENCE

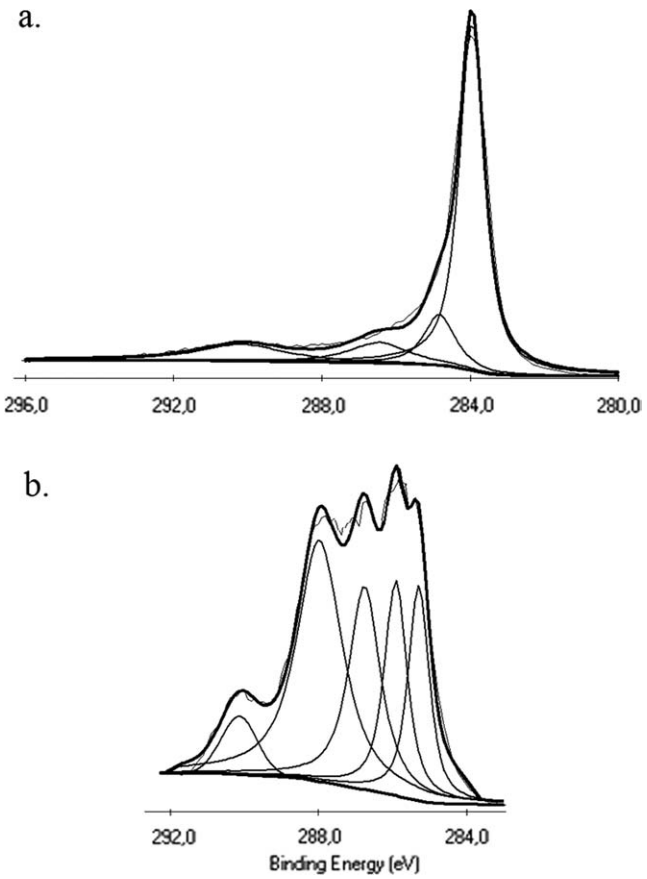

Figure 4. XPS spectra of (a) pristine CNT and (b) PGMA-CNT.

intensity peak at 284.1 eV is assigned to sp^2-hybridized graphite-like carbon atoms.[6] The small peaks at 290.15 and 286.5 eV are due to the —C*=O and —C*—HO bonds of carboxylic acid groups,[6,24] which could be bonded to the nanotube surfaces during nanotube synthesis and purification procedures. The

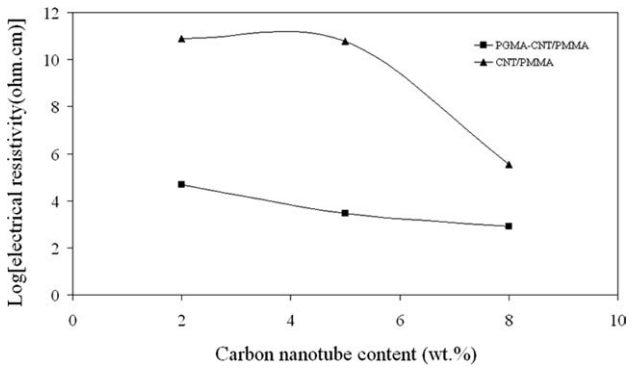

Figure 6. Relationship of CNT content and PGMA-CNT content of PMMA composites with the electrical resistivity values.

peak at 285.2 eV is assigned to sp^3-hybridized dimond-like carbon atoms. XPS survey and high-resolution scans of PGMA-coated nanotubes give totally different bonding states, which indicate a successful coverage of nanotube surfaces by polymer. C/O atomic ratio of 10.1/3 was obtained from survey scan, which is in perfect agreement with the ratio based on the stoichiometry of PGMA (10 : 3). High-resolution C1s spectrum of PGMA-coated nanotubes [Figure 4(b)] can be curve-fitted with five peak components at binding energies (BEs) of 289.15, 287.3, 286.8, 285.9, and 285.0 eV, which can be attributed to —C*=O, —C*H—O—C*H_2—, —O—C*H_2—, —C*(CH_3)—CO—, and —C*H_3 species, respectively.[24,25] The observed BE values for PGMA-coated nanotubes match well with the previously reported results for PGMA.[19,22] Hence, FTIR and XPS analyses support that CNT surfaces are coated by PGMA thin films, which retains the pendant epoxide functional groups. As-deposited films are quite soluble in common organic solvents like acetone and tetrahydofuran (THF), which implies that the films have linear polymeric structure. Film solubility is not desired considering the final purpose of dispersing the nanotubes in organic solvents under harsh ultrasonication

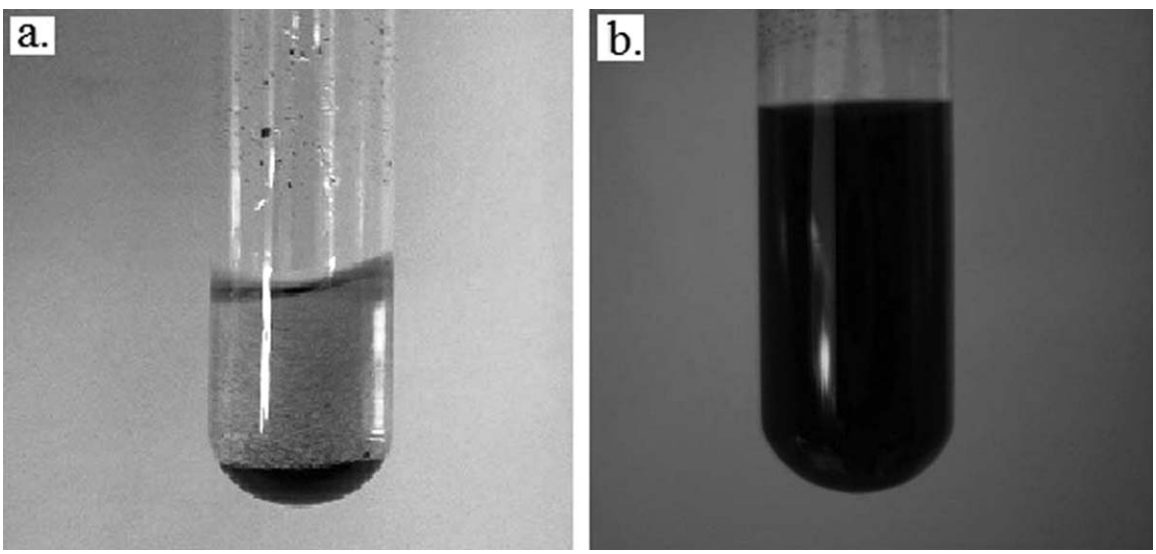

Figure 5. Photographs of the dispersions of (a) Pristine CNT/acetone and (b) PGMA-CNT/acetone suspensions after 6 h and 3 months from ultrasonication, respectively.

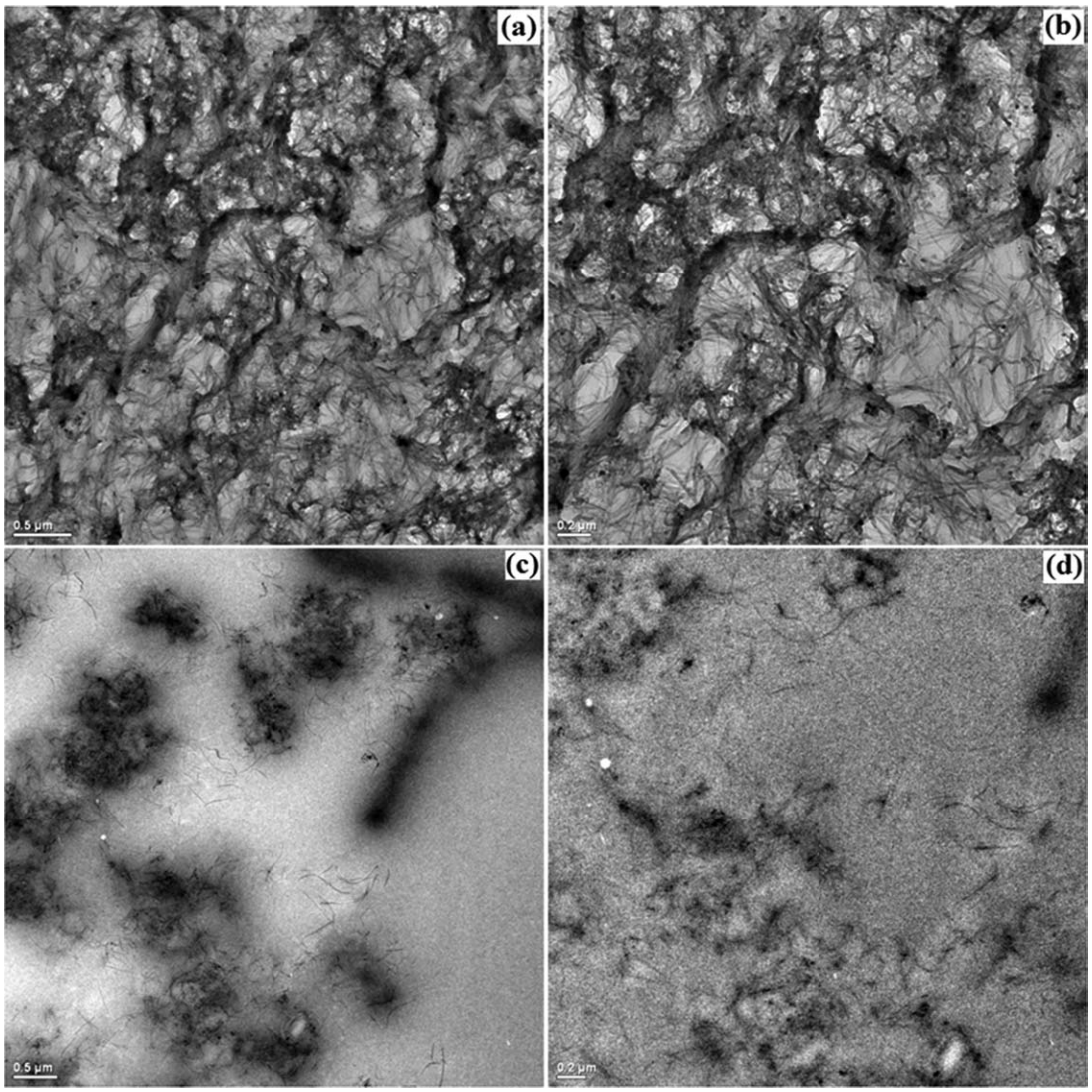

Figure 7. TEM images of PMMA composites including a, b) 2 wt % PGMA-CNT and c, d) pristine CNT.

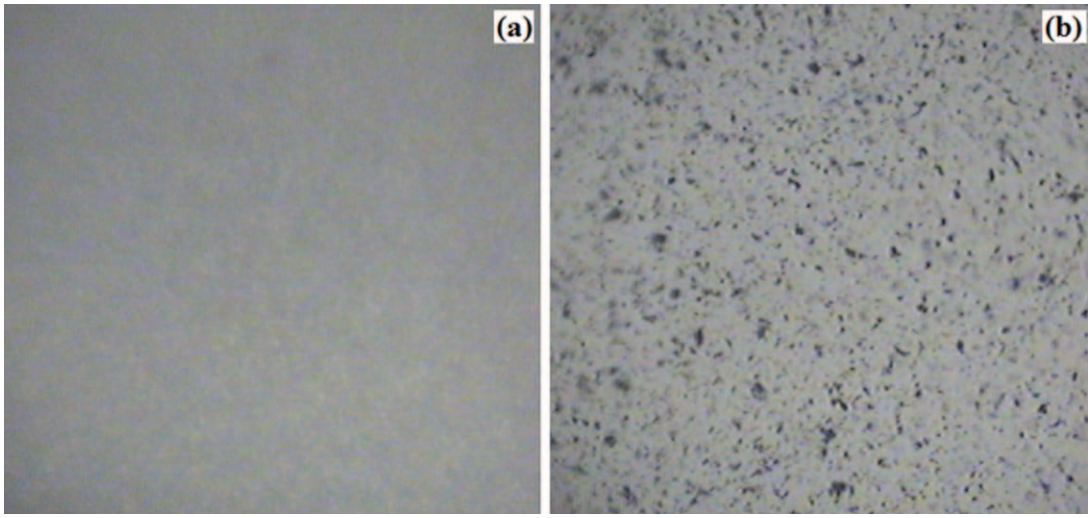

Figure 8. Optical microscopy images of PMMA composites including a) 2 wt % PGMA-CNT and b) pristine CNT. [Color figure can be viewed in the online issue, which is available at wileyonlinelibrary.com.]

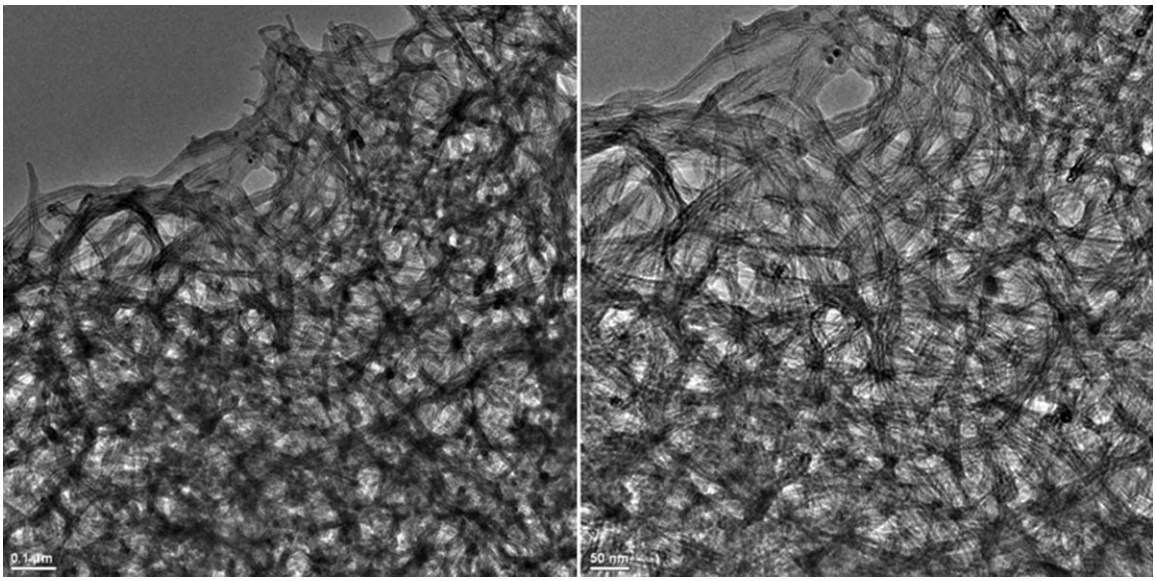

Figure 9. TEM images of PMMA composites including 2 wt % PGMA-CNT.

conditions. To increase the film durability, PGMA films on the CNT surfaces were partially crosslinked during the heat treatment step. It was observed that the heat-treated PGMA-CNT samples were soluble in THF and acetone under ultrasonication conditions, which is an evidence for durable PGMA film on nanotube surfaces.

CNT particles tend to form agglomerate structures unless they are exposed to chemical treatment to reduce the agglomeration tendency by improving the interaction between composite constituents. Figure 5(a) shows the dispersion of untreated CNTs in acetone, after 6 h of ultrasonication. CNT particles tended to form agglomerate structures and settled down in very short time. For the PGMA-functionalized nanotubes [Figure 5(b)], however, a homogeneous, ink-like suspension was observed, and the nanotubes remained suspended for very long times.

Electrical resistivity results of the composite samples prepared from both pristine and functionalized CNTs showed that PGMA-CNT provides lower resistivity compared with uncoated CNTs at the same compositions (Figure 6), which should be the consequence of a decrease in agglomerate size (Figures 7 and 8). PGMA coating of nanotube surfaces by CVD technique before composite preparation improved electrical conductivity by reducing CNT agglomerates and by providing a homogenous distribution of the filler particles in the polymer matrix (Figures 7 and 8). Only better dispersion could not be the reason of improved electrical property. Enhanced distribution without a decrease in agglomerate size would tend to reduce electrical conductivity. As the agglomerate size decreases, the total effective surface area, which was in contact with polymer matrix, of agglomerate particle increases. Hence, decreased particle size resulted to increased particle–particle interaction (Figure 9). Moreover, the distances between CNT particles should be reduced, which led CNT particles to form conductive networks at low concentration (Figure 9).

CNT agglomerates are weak point of composites and should be broken as much as possible. The tensile strength of composite might increase because of a decrease in filler size.[26] Coating of carbon nanoparticles with thin PGMA film prevented agglomeration in PMMA matrix to some extent (Figures 7 and 8), which results an increase in the tensile strength compared to CNT/PMMA (Table I). PGMA-CNT provides also lower electrical resistivity at each composition. Improvement in tensile strength and electrical property should be the result of the same effect. Although the surface of CNTs is quite inert, the coating of PGMA film containing various polar groups may form strong covalent bonds with the carbonyl groups of PMMA.[27] The PGMA coating together with the ultrahigh surface area of CNTs

Table I. Tensile Properties of Poly(methyl methacrylate) Composites Containing Pristine CNT and PGMA-CNT with (±) Standard Deviations

Material	Tensile strength (MPa)	Tensile modulus (MPa)	Elongation at break (%)
PMMA	48.5 ± 0.9	918 ± 48	9.7 ± 0.5
PMMA composite with including 2 wt % CNT	29.5 ± 4.8	1150 ± 216	5.3 ± 1.4
PMMA composite with including 2 wt % PGMA-CNT	53.1 ± 3.8	1319 ± 157	8.2 ± 1.1
PMMA composite with including 5 wt % CNT	23.6 ± 3.6	1208 ± 224	4.4 ± 0.4
PMMA composite with including 5 wt % PGMA-CNT	48.3 ± 2.5	1784 ± 179	5.7 ± 0.3
PMMA composite with including 8 wt % CNT	23.4 ± 2.6	1572 ± 184	2.8 ± 0.6
PMMA composite with including 8 wt % PGMA-CNT	40.1 ± 1.5	1945 ± 93	3.9 ± 0.4

causes a substantial interface region and strong interactions with the polymer to alter the tensile property of the polymer.[27]

The addition of CNTs increases the modulus of prepared composites due to the rigid character of this filler.[26] Tensile modulus values of filled composites obtained from uncoated and PGMA-coated CNTs are different from each other (Table I), which might be the consequence of the difference in agglomerate size of carbon nanoparticles (Figures 7 and 8). Compared with uncoated CNTs-containing composites, PGMA-CNT/PMMA showed higher tensile modulus values, which suggest the good reinforcement effect of the PGMA-CNT.[27] The lack of inherent chemical interaction between uncoated CNTs and PMMA leads to the limited reinforcement in modulus of uncoated carbon nanoparticles[18] and prevents effective load transfer.[28] Elongation at break values (Table I) of both CNT/PMMA and PGMA-CNT/PMMA composites is quite low because CNT agglomerates are large enough to form critical defects resulting in stress concentration in the polymer, which causes the brittle behavior. PGMA-CNT/PMMA test samples elongate more compared with untreated CNTs-filled composites, which might be due to the plasticizing effect of thin PGMA coatings on CNTs.

CONCLUSIONS

Thin PGMA polymer film was coated conformally on CNT surfaces. PMMA composites prepared by PGMA-coated CNTs showed lower electrical resistivity and enhanced tensile properties at each composition of the nanoparticle when compared with the composites, including uncoated CNTs. This improvement should be the result of a decrease in agglomerate size of CNTs in the polymer matrix in the presence of the chemical interaction between PGMA-coated CNTs and PMMA.

ACKNOWLEDGMENTS

This research was supported by the Scientific and Technological Research Council of Turkey (TUBITAK) (Project No. 109M763).

REFERENCES

1. Baughman, R. H.; Zakhidov, A. A.; Heer, W. A. *Science* **2000,** *297*, 787.
2. Sarangapani, S.; Lessner, P.; Forchione, J.; Griffith, A.; Laconti, A. B. *J. Power Sources* **1990,** *29*, 355.
3. Zhang, N.; Xie, J.; Varadan V. K. *Smart Mater. Struct.* **2006,** *15*, 123.
4. Koysuren, O.; Du, C.; Pan, N.; Bayram, G. J. *Appl. Polym. Sci.* **2009,** *113*, 1070.
5. Gorga, R. E.; Lau, K. K. S.; Gleason, K. K.; Cohen, R. E. *J. Appl. Polym. Sci.* **2006,** *102*, 1413.
6. Kim, J. A.; Seong, D. G.; Kang, T. J.; Youn, J. R. *Carbon* **2006,** *44*, 1898.
7. Xie, X. L.; Mai, Y. W.; Zhou, X. P. *Mater. Sci. Eng. R* **2005,** *49*, 89.
8. Spitalsky, Z.; Tasis, D.; Papagelis, K.; Galiotis, C. *Prog. Polym. Sci.* **2010,** *35*, 357.
9. Wong, K. K. H.; Zinke-Allmang, M.; Hutter, J. L.; Hrapovic, S.; Luong, J. H. T.; Wan, W. *Carbon* **2009,** *47*, 2571.
10. Jeon, H. J.; Youk, J. H.; Yu, W. R. *Macromol. Res.* **2010,** *18*, 458.
11. Cao, L.; Chen, H. Z.; Wang, M.; Sun, J. Z. *J. Phys. Chem. B* **2002,** *106*, 8971.
12. Wang, M.; Pramoda, K. P.; Goh, S. H. *Polymer* **2005,** *46*, 11510.
13. Liu, Y. L.; Chen, W. H. *Macromolecules* **2007,** *40*, 8881.
14. Sobkowicz, M. J.; White, E. A.; Dorgan, J. R. *J. Appl. Polym. Sci.* **2011,** *122*, 2563.
15. Gao, C.; Vo, C. D.; Jin, Y. Z.; Li, W.; Armes, S. P. *Macromolecules* **2005,** *38*, 8634.
16. Asatekin, A.; Barr, M. C.; Baxamusa, S. H.; Lau, K. K. S.; Tenhaeff, W.; Xu, J.; Gleason, K. K. *Mater. Today* **2010,** *13*, 26.
17. Karaman, M.; Kooi, S.; Gleason, K. K. *Chem. Mater.* **2008,** *20*, 2262.
18. Du, C.; Yeh, J.; Pan, N. *Nanotechnology* **2005,** *16*, 350.
19. Lau, K. K. S.; Gleason, K. K. *Adv. Mater.* **2006,** *18*, 1972.
20. Wei, H.; Hsiue, G.; Liu, C. *Compos. Sci. Technol.* **2007,** *67*, 1018.
21. Vatsman, L.; Marom, G.; Wagner, H. D. *Adv. Func. Mater.* **2006,** *16*, 357.
22. Mao, Y.; Gleason K. K. *Langmuir* **2004,** *20*, 2484.
23. Coblentz Society, Inc., Evaluated Infrared Reference Spectra, in NIST Chemistry WebBook, NIST Standard Reference Database Number 69; Linstrom, P. J., Mallard, W. G., Eds.; National Institute of Standards and Technology: Gaithersburg MD, 20899. Available at: http://webbook.nist.gov, accessed on April, **2012.**
24. NIST X-ray Photoelectron Spectroscopy Database, Version 3.5 (National Institute of Standards and Technology, Gaithersburg, **2003**). Available at: http://srdata.nist.gov/xps/, accessed on April, **2012.**
25. Beamson, G.; Briggs, D. High Resolution XPS of Organic Polymers: the Scienta ESCA300 Database; Wiley: Chichester, UK, **1992.**
26. Nielsen, L. E.; Landel, R. F. Mechanical Properties of Polymer and Composites; Marcel Dekker: New York, **1994.**
27. Wang, Y.; ZiXing, S.; Yin, J. *Polymer* **2011,** *52*, 3661.
28. Cooper, C. A.; Ravich, D.; Lips, D.; Mayer, J.; Wagner, D. *Compos. Sci. Technol.* **2002,** *62*, 1105.